

# Search for three-nucleon short-range correlations in light nuclei

Z. Ye,<sup>1,2,3</sup> P. Solvignon,<sup>4,5,\*</sup> D. Nguyen,<sup>2</sup> P. Aguilera,<sup>6</sup> Z. Ahmed,<sup>7</sup> H. Albataineh,<sup>8</sup> K. Allada,<sup>5</sup> B. Anderson,<sup>9</sup> D. Anez,<sup>10</sup> K. Aniol,<sup>11</sup> J. Annand,<sup>12</sup> J. Arrington,<sup>1</sup> T. Averett,<sup>13</sup> H. Baghdasaryan,<sup>2</sup> X. Bai,<sup>14</sup> A. Beck,<sup>15</sup> S. Beck,<sup>15</sup> V. Bellini,<sup>16</sup> F. Benmokhtar,<sup>17</sup> A. Camsonne,<sup>5</sup> C. Chen,<sup>18</sup> J.-P. Chen,<sup>5</sup> K. Chirapatpimol,<sup>2</sup> E. Cisbani,<sup>19</sup> M. M. Dalton,<sup>2,5</sup> A. Daniel,<sup>20</sup> D. Day,<sup>2</sup> W. Deconinck,<sup>21</sup> M. Defurne,<sup>22</sup> D. Flay,<sup>23</sup> N. Fomin,<sup>24</sup> M. Friend,<sup>25</sup> S. Frullani,<sup>19</sup> E. Fuchey,<sup>23</sup> F. Garibaldi,<sup>19</sup> D. Gaskell,<sup>5</sup> S. Gilad,<sup>21</sup> R. Gilman,<sup>26</sup> S. Glamazdin,<sup>27</sup> C. Gu,<sup>2</sup> P. Guèye,<sup>18</sup> C. Hanretty,<sup>2</sup> J.-O. Hansen,<sup>5</sup> M. Hashemi Shabestari,<sup>2</sup> O. Hen,<sup>28</sup> D. W. Higinbotham,<sup>5</sup> M. Huang,<sup>3</sup> S. Iqbal,<sup>11</sup> G. Jin,<sup>2</sup> N. Kalantarians,<sup>2</sup> H. Kang,<sup>29</sup> A. Kelleher,<sup>21</sup> I. Korover,<sup>28</sup> J. LeRose,<sup>5</sup> J. Leckey,<sup>30</sup> R. Lindgren,<sup>2</sup> E. Long,<sup>9</sup> J. Mammei,<sup>31</sup> D. J. Margaziotis,<sup>11</sup> P. Markowitz,<sup>32</sup> D. Meekins,<sup>5</sup> Z. Meziani,<sup>23</sup> R. Michaels,<sup>5</sup> M. Mihovilovic,<sup>33</sup> N. Muangma,<sup>21</sup> C. Munoz Camacho,<sup>34</sup> B. Norum,<sup>2</sup> Nuruzzaman,<sup>35</sup> K. Pan,<sup>21</sup> S. Phillips,<sup>4</sup> E. Piasetzky,<sup>28</sup> I. Pomerantz,<sup>28,36</sup> M. Posik,<sup>23</sup> V. Punjabi,<sup>37</sup> X. Qian,<sup>3</sup> Y. Qiang,<sup>5</sup> X. Qiu,<sup>38</sup> P. E. Reimer,<sup>1</sup> A. Rakhman,<sup>7</sup> S. Riordan,<sup>2,39</sup> G. Ron,<sup>40</sup> O. Rondon-Aramayo,<sup>2</sup> A. Saha,<sup>5,\*</sup> L. Selvy,<sup>9</sup> A. Shahinyan,<sup>41</sup> R. Shneur,<sup>28</sup> S. Sirca,<sup>42,33</sup> K. Slifer,<sup>4</sup> N. Sparveris,<sup>23</sup> R. Subedi,<sup>2</sup> V. Sulkosky,<sup>21</sup> D. Wang,<sup>2</sup> J. W. Watson,<sup>9</sup> L. B. Weinstein,<sup>8</sup> B. Wojtsekhowski,<sup>5</sup> S. A. Wood,<sup>5</sup> I. Yaron,<sup>28</sup> X. Zhan,<sup>1</sup> J. Zhang,<sup>5</sup> Y. W. Zhang,<sup>26</sup> B. Zhao,<sup>13</sup> X. Zheng,<sup>2</sup> P. Zhu,<sup>43</sup> and R. Zielinski<sup>4</sup>

(The Jefferson Lab Hall A Collaboration)

<sup>1</sup>*Physics Division, Argonne National Laboratory, Argonne, IL 60439*

<sup>2</sup>*University of Virginia, Charlottesville, VA 22904*

<sup>3</sup>*Duke University, Durham, NC 27708*

<sup>4</sup>*University of New Hampshire, Durham, NH 03824*

<sup>5</sup>*Thomas Jefferson National Accelerator Facility, Newport News, VA 23606*

<sup>6</sup>*Institut de Physique Nucléaire (UMR 8608), CNRS/IN2P3 - Université Paris-Sud, F-91406 Orsay Cedex, France*

<sup>7</sup>*Syracuse University, Syracuse, NY 13244*

<sup>8</sup>*Old Dominion University, Norfolk, VA 23529*

<sup>9</sup>*Kent State University, Kent, OH 44242*

<sup>10</sup>*Saint Mary's University, Halifax, Nova Scotia, Canada*

<sup>11</sup>*California State University, Los Angeles, Los Angeles, CA 90032*

<sup>12</sup>*University of Glasgow, Glasgow G12 8QQ, Scotland, United Kingdom*

<sup>13</sup>*College of William and Mary, Williamsburg, VA 23187*

<sup>14</sup>*China Institute of Atomic Energy, Beijing, China*

<sup>15</sup>*Nuclear Research Center Negev, Beer-Sheva, Israel*

<sup>16</sup>*Universita di Catania, Catania, Italy*

<sup>17</sup>*Duquesne University, Pittsburgh, PA 15282*

<sup>18</sup>*Hampton University, Hampton, VA 23668*

<sup>19</sup>*INFN, Sezione Sanità and Istituto Superiore di Sanità, 00161 Rome, Italy\**

<sup>20</sup>*Ohio University, Athens, OH 45701*

<sup>21</sup>*Massachusetts Institute of Technology, Cambridge, MA 02139*

<sup>22</sup>*CEA Saclay, F-91191 Gif-sur-Yvette, France*

<sup>23</sup>*Temple University, Philadelphia, PA 19122*

<sup>24</sup>*University of Tennessee, Knoxville, TN 37996*

<sup>25</sup>*Carnegie Mellon University, Pittsburgh, PA 15213*

<sup>26</sup>*Rutgers, The State University of New Jersey, Piscataway, NJ 08855*

<sup>27</sup>*Kharkov Institute of Physics and Technology, Kharkov 61108, Ukraine*

<sup>28</sup>*Tel Aviv University, Tel Aviv 69978, Israel*

<sup>29</sup>*Seoul National University, Seoul, Korea*

<sup>30</sup>*Indiana University, Bloomington, IN 47405*

<sup>31</sup>*Virginia Polytechnic Inst. and State Univ., Blacksburg, VA 24061*

<sup>32</sup>*Florida International University, Miami, FL 33199*

<sup>33</sup>*Jozef Stefan Institute, Ljubljana, Slovenia*

<sup>34</sup>*Université Blaise Pascal/IN2P3, F-63177 Aubièrre, France*

<sup>35</sup>*Mississippi State University, Mississippi State, MS 39762*

<sup>36</sup>*The University of Texas at Austin, Austin, Texas 78712*

<sup>37</sup>*Norfolk State University, Norfolk, VA 23504*

<sup>38</sup>*Lanzhou University, Lanzhou, China*

<sup>39</sup>*University of Massachusetts, Amherst, MA 01006*

<sup>40</sup>*Racah Institute of Physics, Hebrew University of Jerusalem, Jerusalem, Israel*

<sup>41</sup>*Yerevan Physics Institute, Yerevan 375036, Armenia*

<sup>42</sup>*Faculty of Mathematics and Physics, University of Ljubljana, Ljubljana, Slovenia*

<sup>43</sup>*University of Science and Technology, Hefei, China*

(Dated: June 10, 2022)

We present new data probing short-range correlations (SRCs) in nuclei through the measurement of electron scattering off high-momentum nucleons in nuclei. The inclusive  ${}^4\text{He}/{}^3\text{He}$  cross section ratio is observed to be both  $x$  and  $Q^2$  independent for  $1.5 < x < 2$ , confirming the dominance of two-nucleon (2N) short-range correlations (SRCs). For  $x > 2$ , our data do not support a previous claim of three-nucleon (3N) correlation dominance. While contributions beyond those from stationary 2N-SRCs are observed, our data show that isolating 3N-SRCs is more complicated than for 2N-SRCs.

PACS numbers: 13.60.Hb, 25.10.+s, 25.30.Fj

Understanding the complex structure of the nucleus remains one of the major uncompleted tasks in nuclear physics, and the high-momentum components of the nuclear wave-function continue to attract attention [1–3]. Momenta above the Fermi momentum are strongly suppressed in shell model and mean field calculations [4]. Subsequently, these calculations under-predict (over-predict) the cross section for proton knock-out reactions above (below) the Fermi momentum [5–7].

In the dense and energetic environment of the nucleus, nucleons have a significant probability of interacting at distances  $\leq 1$  fm, even in light nuclei [8]. Protons and neutrons interacting through the strong, short-distance part of the nucleon-nucleon (NN) interaction give rise to pairs of nucleons with large relative momenta. These short-range correlations (SRCs) are an important source of high-momentum nucleons in nuclei [1–3, 9, 10]. These are the primary source of nucleons above the Fermi momentum,  $k_F \approx 250\text{--}300$  MeV/c, associated with the shell model picture of nuclear structure. For momenta below  $k_F$ , we observe shell-model behavior which is strongly  $A$  dependent, while two-body physics dominates above  $k_F$  resulting in a universal structure for all nuclei that is driven by the details of the NN interaction [11–13].

In the case of inclusive electron-nucleus scattering, it is possible to isolate scattering from high-momentum nucleons in specific kinematic regions. The electron transfers energy,  $\nu$ , and momentum,  $\vec{q}$ , to the struck nucleon by exchanging a virtual photon with four momentum transfer  $q^2 = -Q^2 = \nu^2 - |\vec{q}|^2$ . It is useful in this case to define the kinematic variable  $x = Q^2/(2M_p\nu)$ , where  $M_p$  is the mass of the proton. Elastic scattering from a stationary proton corresponds to  $x = 1$ , while inelastic scattering must occur at  $x < 1$  and scattering at  $x > 1$  is kinematically forbidden. In a nucleus, the momentum of the nucleon produces a broadened quasielastic peak centered near  $x = 1$ . At values of  $x$  slightly greater than unity, scattering can only occur from nucleons with non-zero momentum. As  $x$  increases, larger initial momenta are required until scattering from nucleons below the Fermi momentum is kinematically forbidden, isolating scattering from high-momentum nucleons associated with SRCs [1, 11, 12].

Because the momentum distribution of the nucleus is not a physical observable, one cannot directly extract and study its high-momentum component. One can, however, test the idea of a universal structure at high-momenta by

comparing scattering from different nuclei at kinematics which require that the struck nucleon have a high initial momentum [11]. Previous measurements at SLAC and Jefferson Lab revealed a universal form to the scattering in the region dominated by high-momentum nucleons [1, 10, 14–18]. In these experiments, the cross section ratios for inclusive scattering from heavy nuclei to the deuteron were shown to scale, i.e. be independent of  $x$  and  $Q^2$ , for  $x \gtrsim 1.5$  and  $Q^2 \gtrsim 1.5$  GeV<sup>2</sup>, corresponding to scattering from nucleons with momenta above 300 MeV/c. Other measurements have demonstrated that these high-momentum components are dominated by high-momentum n-p pairs [19–24], suggesting that these components have a predominantly deuteron-like structure in all nuclei. While final-state interactions (FSI) decrease with increasing  $Q^2$  in inclusive scattering, FSI between nucleons in the correlated pair may not disappear. It is typically assumed that the FSI are identical for the deuteron and the deuteron-like pair in heavier nuclei, and thus cancel in these ratios [1, 11].

This approach can be extended to look for universal behavior arising from 3N-SRCs by examining scattering at  $x > 2$ , beyond the kinematic limit for scattering from a deuteron. Within the simple SRC model [9, 10], the cross section is composed of scattering from one-body, two-body, etc... configurations, with the one-body (shell-model) contributions dominating at  $x \approx 1$ , while 2N(3N)-SRCs dominate as  $x \rightarrow 2(3)$ . Taking ratios of heavier nuclei to  ${}^3\text{He}$  allows a similar examination of the target ratios for  $x > 2$ , where the simple SRC model predicts a universal behavior associated with three-nucleon SRCs (3N-SRCs) - configurations where three nucleons have large relative momenta but little total momentum. 3N-SRCs could come from either three-nucleon forces or multiple hard two-nucleon interactions. The first such measurement [15] observed  $x$ -independent ratios for  $x > 2.25$  at modest  $Q^2$  values, which was interpreted as a result of 3N-SRCs dominance in this region. However, the plateau in  $x$  was only shown for ratios averaged over the full  $Q^2$  range of the measurement; there was no demonstration that the plateau persisted over a range in  $Q^2$ . A later measurement of the  ${}^4\text{He}/{}^3\text{He}$  ratios at larger  $Q^2$  values [16] were found to be significantly larger and did not show a clear plateau in  $x$ . Consequently, the question of whether 3N-SRC contributions have been cleanly identified and observed to dominate at large  $x$  is as yet unanswered.

The results reported here are from JLab experiment E08-014 [25], which focused on precise measurements of the  $x$  and  $Q^2$  dependence of the  ${}^4\text{He}/{}^3\text{He}$  cross section ratios at large  $x$ . A 3.356 GeV electron beam with currents ranging from 40 to 120  $\mu\text{A}$  impinged on nuclear targets, and scattered electrons were detected in two nearly identical High-Resolution Spectrometers (HRSs) [26]. Data were taken on three 20-cm long cryogenic targets (liquid  ${}^2\text{H}$  and gaseous  ${}^3\text{He}$  and  ${}^4\text{He}$ ) and thin foils of  ${}^{12}\text{C}$  and  ${}^{40,48}\text{Ca}$ . We focus here on the  ${}^{3,4}\text{He}$  data acquired to study the 3N-SRC region. The Calcium data were taken to examine isospin dependence of 2N-SRCs and will be the subject of a subsequent paper.

Each HRS consists of a pair of vertical drift chambers (VDCs) for particle tracking, two scintillator planes for triggering and timing measurements, a gas Čerenkov counter, and two layers of lead-glass calorimeters for particle identification [26]. Scattering was measured at  $\theta = 21^\circ, 23^\circ, 25^\circ$ , and  $28^\circ$ , covering a  $Q^2$  range of 1.3–2.2  $\text{GeV}^2$ . A detailed description of the experiment and data analysis can be found in Ref. [27].

The data analysis is relatively straightforward, as inclusive scattering at  $x > 1$  yields modest rates and a small pion background. The trigger and tracking inefficiencies are small and applied as a correction to the measured yield. Electrons are identified by applying cuts on the signals from both the Čerenkov detector and the calorimeters. The cuts give  $> 99\%$  electron efficiency with negligible pion contamination. The overall dead-time of the data acquisition system was evaluated on a run-by-run bases. To ensure a well-understood acceptance, the solid angle and momentum were limited to high-acceptance regions and a model of the HRSs was used to apply residual corrections [27].

The scattered electron momentum, in-plane and out-of-plane angles, and vertex position at the target can be reconstructed from the VDC tracking information. The transformation from focal plane to target quantities has been obtained from previous experiments, but for the right HRS, the third quadrupole could not achieve its nominal operating current and was operated at 85% of its nominal field for all kinematics. New optics data were taken to correct for the modified tune. Many of the systematic uncertainties in the spectrometers are correlated, and so when merging data from the two spectrometers, we add the statistics and then apply the systematic uncertainties to the combined result.

The  ${}^{3,4}\text{He}$  targets have a large background from scattering in the cell walls. We apply a  $\pm 7$  cm cut around the center of the target, removing  $> 99.9\%$  of the events from target endcap scattering, as determined from measurements on empty target cells. One of the largest contributions to the systematic uncertainty comes from target density reduction due to heating of the  ${}^2\text{H}$ ,  ${}^3\text{He}$ , and  ${}^4\text{He}$  targets by the high-current electron beam. We made dedicated measurements over a range of beam currents

and used the variation of the yield to evaluate the effect of beam current on the target density. We observed a large current dependence that was not constant over the target length, and the extrapolation to zero current did not yield a uniform density. This indicates a non-linear current dependence that is not uniform along the length of the target, making it difficult to determine the absolute target thickness. However, the observed heating effects were very similar in  ${}^3\text{He}$  and  ${}^4\text{He}$ , and the  ${}^4\text{He}/{}^3\text{He}$  ratios are consistent with previous data near the quasielastic peak and in the 2N-SRC region. We therefore assume that the error in extrapolating to zero current largely cancels in the ratio and apply a 5% scale uncertainty for the  ${}^4\text{He}/{}^3\text{He}$  ratios. For the absolute uncertainty, the  ${}^{3,4}\text{He}$  targets have a large normalization uncertainty, potentially 10% or larger. This normalization uncertainty does not impact our study of 3N-SRCs, and so we do not attempt to normalize the data to existing measurements, but it is a significant issue for comparisons of the solid targets to  ${}^2\text{H}$  or  ${}^3\text{He}$ . These ratios have an additional complication arising from the fact that the rapidly falling cross sections makes the extraction sensitive to the resolution, and the resolution is somewhat different for the short and long targets. These issues are being examined, but in the present work we focus on precise comparisons of the nearly-identical  ${}^3\text{He}$  and  ${}^4\text{He}$  targets.

The measured yield, corrected for inefficiencies and normalized to the integrated luminosity, were binned in  $x$  and compared to simulated yields. The simulation uses a  $y$ -scaling cross section model [17, 28] with radiative corrections computed using the peaking approximation [29]. Coulomb corrections are applied within an improved effective momentum approximation [30, 31], and are 2% or smaller for all data presented here. The uncertainty in the target thicknesses dominates the total scale uncertainty (5.1%) of the ratios, while density fluctuations and dummy subtraction dominate the point-to-point systematic uncertainty of 1.3%.

Figure 1 presents the  ${}^4\text{He}/{}^3\text{He}$  cross section ratio for measurements with  $Q^2 > 1.4 \text{ GeV}^2$ , obtained by combining the data from  $23^\circ$  and  $25^\circ$  scattering. In the 2N-SRC region, our data are in good agreement with the JLab CLAS [15] and Hall C [16] measurements, revealing a plateau for  $1.5 < x < 2$ . At  $x > 2$ , our ratios are significantly larger than the CLAS data, but consistent with the Hall C results. This supports the explanation provided in a recent comment [32] which concluded that the observed plateau was likely the result of large bin-migration effects resulting from the limited CLAS momentum resolution.

While the rise in the ratio above  $x = 2$  may indicate contributions beyond 2N-SRCs, we do not observe the 3N-SRC plateau expected in the naive SRC model [9, 10]. The prediction of scaling as an indication of SRC dominance is a simple and robust way to test for 2N-SRCs. However, it is much less clear how well it can indicate the

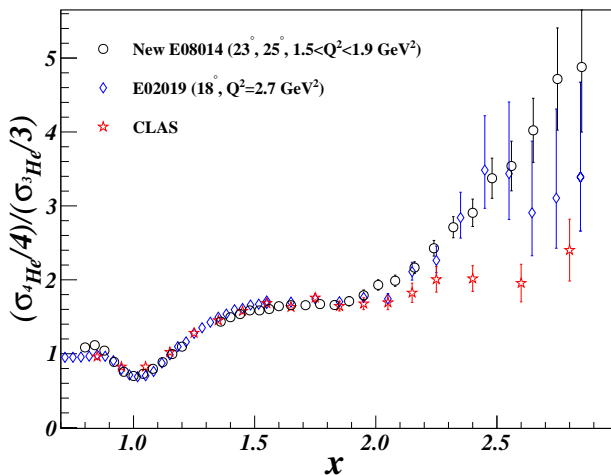


FIG. 1. (Color online) The  ${}^4\text{He}/{}^3\text{He}$  normalized cross section ratio for  $Q^2 > 1.4 \text{ GeV}^2$ , along with previous JLab ratios from CLAS [15] and Hall C (E02-019) [16] (slightly offset in  $x$  for clarity). Error bars include statistical and systematic uncertainties; the 5.1% scale uncertainty is not shown.

presence of 3N-SRCs. For 2N-SRCs, one can predict *a priori* where the plateau should be observed: for a given  $Q^2$  value,  $x$  can be chosen to require a minimum nucleon momentum above the Fermi momentum, strongly suppressing single-particle contributions. It is not clear what values of  $x$  and  $Q^2$  are required to suppress 2N-SRC contributions well enough to isolate 3N-SRCs. Much larger  $Q^2$  values may be required to isolate 3N-SRCs and see analogous plateaus at  $x > 2.5$  [2].

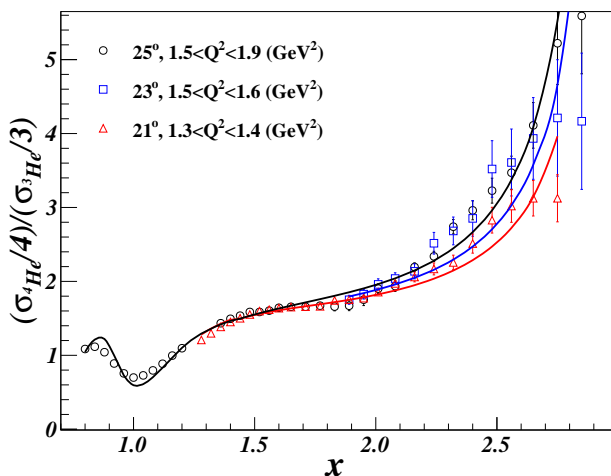


FIG. 2. (Color online) Our  ${}^4\text{He}/{}^3\text{He}$  normalized cross section ratios for all angles. The solid lines are ratios from our  $y$ -scaling cross section model based on a parameterized longitudinal momentum distribution  $F(y)$ . The 5.1% normalization uncertainty is not shown.

For  $A/{}^2\text{H}$  ratios, the plateau must eventually dis-

appear as the deuteron cross section falls to zero for  $x \rightarrow M_D/M_p \approx 2$ , causing the ratio to rise sharply to infinity. Both the previous high- $Q^2$  deuterium data and our simple cross section model show that the sharp drop of the deuteron cross section does not occur until  $x \approx 1.9$ , resulting in a clear plateau for  $1.5 < x < 1.9$ . For  ${}^3\text{He}$ , our cross section starting model shows a similar falloff of the  ${}^3\text{He}$  cross section starting near  $x \approx 2.5$ , producing a rise in the  $A/{}^3\text{He}$  ratio that sets in well below the kinematic limit  $x \approx 3$ . This rapid rise in the  $A/{}^3\text{He}$  ratio as one approaches the  ${}^3\text{He}$  kinematic threshold shifts to lower  $x$  as  $Q^2$  increases, as seen in Fig 2. Note that the cross section is based on a  $y$ -scaling model with a  $Q^2$ -independent longitudinal momentum distribution, so the  $Q^2$  dependence in the rise of the plateau at  $x > 2.5$  comes only from the  $Q^2$  dependence in the approach to the kinematic threshold. While the low- $x$  side of the plateau is expected to set in at lower  $x$  values as  $Q^2$  increases, as seen in the 2N-SRC region [10], the large- $x$  breakdown as  $x$  approaches the kinematic limit for  ${}^3\text{He}$  also shifts to lower  $x$  values, potentially limiting the  $x$  range over which a plateau could be observed, even in the case of 3N-SRC dominance.

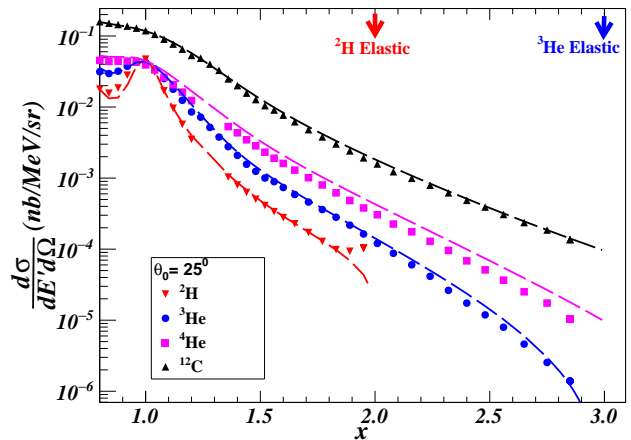


FIG. 3. (Color online) Cross sections of  ${}^2\text{H}$ ,  ${}^3\text{He}$ ,  ${}^4\text{He}$  and  ${}^{12}\text{C}$  at  $25^\circ$ ; note that the rise in deuterium near  $x = 2$  is the deuteron elastic scattering contribution. Only statistical uncertainties are shown.

The inclusive cross sections for  ${}^2\text{H}$ ,  ${}^3\text{He}$ ,  ${}^4\text{He}$  and  ${}^{12}\text{C}$  at a scattering angle of  $25^\circ$  are shown in Figure 3. The  ${}^3\text{He}$  cross section falls more rapidly than the other nuclei for  $x > 2.5$ , yielding the rise in the  ${}^4\text{He}/{}^3\text{He}$  ratios discussed above. In the naive SRC model, it is assumed that the high- $x$  cross section comes from the contributions of *stationary* 2N- and 3N-SRCs. Motion of 2N(3N)-SRCs in  $A > 2(3)$  nuclei means that the contributions from these SRCs will not be identical in all nuclei, and so the prediction of identical behavior (and thus perfect scaling) breaks down, though approximate scaling may persist if the impact of the SRC motion is not too large. For

the most recent extraction of 2N-SRCs from the  $A/{}^2\text{H}$  ratios [16], the effect of the 2N-SRC motion in heavier nuclei was estimated and found to give a small enhancement of the ratio in the plateau region, with relatively small distortion of the shape until  $x > 1.9$  where the ratio increases rapidly to infinity [12, 16].

We have performed high-statistics measurements of the  ${}^4\text{He}/{}^3\text{He}$  cross section ratio over a range of  $Q^2$ , confirming the results of the low-statistics measurements from Hall C [16] and showing a clear disagreement with the CLAS data [15] for  $x > 2$ . This supports the idea that the large- $x$  CLAS data were limited by bin-migration effects due to the spectrometer's modest momentum resolution [32]. We do not observe the plateau predicted by the naive SRC model, but show why the prediction of scaling in the 3N-SRC regime is not as robust as for 2N-SRC. For 2N-SRCs, the impact of SRC motion is large only for  $x > 1.9$ , as the cross section drops rapidly approaching the kinematic threshold. For 3N-SRCs, the cross section deviates from the roughly uniform falloff with  $x$  much earlier, enhancing the impact of SRC motion. Even if 3N-SRC contributions dominate the cross section, the scaling predicted assuming stationary 3N-SRCs may be violated.

While our  ${}^4\text{He}/{}^3\text{He}$  ratios do not provide indication of 3N-SRCs, this does not indicate that they are not important in this region, and it should still be possible to use inclusive scattering to look for contributions of 3N configurations in nuclei. The biggest obstacle appears to be the need for larger  $Q^2$  and the fact that the plateau region may be significantly narrower for 3N-SRCs than is observed for 2N-SRCs. Larger  $Q^2$  values may be sufficient to isolate 3N-SRCs. Alternatively, one could compare the  ${}^3\text{He}$  cross section at large  $x$  with a model of the contributions of moving 2N-SRCs in  ${}^3\text{He}$ . A significant 3N-SRC contribution would increase the cross section relative to what is expected when modeling scattering from  ${}^3\text{He}$  in terms of single-particle and 2N-SRC contributions. However, because this is a comparison to theory, rather than a comparison of SRCs within two nuclei, one can no longer rely on final-state interactions canceling in the comparison, and these effects would also have to be modeled.

It will be important for such comparisons to be performed over a range of  $Q^2$ , making data to be taken at Jefferson Lab [33] important for such studies. If 3N-SRC contributions are found to be significant, it will also be important to address the question of their isospin dependence. The prediction of scaling in the  $A/{}^3\text{He}$  ratios also assumes that all 3N-SRCs have the same isospin structure as  ${}^3\text{He}$ , or that the  $x$  and  $Q^2$  dependence are identical for all significant 3N-SRCs contributions. Planned measurements of scattering from  ${}^3\text{He}$  and  ${}^3\text{H}$  at large  $x$  [34] will provide a direct comparison of the high- $x$  contributions from ppn- and pnn-SRCs, important for quantitative interpretation of future  $A/{}^3\text{He}$  ratios.

We acknowledge the outstanding support from the

Jefferson Lab Hall A technical staff and the JLab target group. This work was supported in part by the DOE Office of Science, Office of Nuclear Physics, contract DE-AC05-06OR23177, under which JSA, LLC operates JLab, DOE contracts DE-AC02-06CH11357 and DE-FG02-96ER40950, the National Science Foundation, and the UK Science and Technology Facilities Council (ST/J000175/1,ST/G008604/1).

---

\* deceased

- [1] J. Arrington, D. Higinbotham, G. Rosner, and M. Sargsian, *Prog. Part. Nucl. Phys.* **67**, 898 (2012).
- [2] N. Fomin, D. Higinbotham, M. Sargsian, and P. Solvignon, *Ann. Rev. Nucl. Part. Sci.* **67**, 2115 (2017).
- [3] O. Hen, G. A. Miller, E. Piassetzky, and L. B. Weinstein, *Rev. Mod. Phys.* **89**, 045002 (2017).
- [4] T. DeForest, *Nucl. Phys.* **A392**, 232 (1983).
- [5] G. Van Der Steenhoven *et al.*, *Nucl. Phys.* **A480**, 547 (1988).
- [6] L. Lapikas, *Nucl. Phys. A* **553**, 297 (1993).
- [7] J. Kelly, *Adv. Nucl. Phys.* **23**, 75 (1996).
- [8] J. Carlson *et al.*, (2014), 1412.3081.
- [9] L. Frankfurt and M. Strikman, *Physics Reports* **76**, 215 (1981).
- [10] L. L. Frankfurt, M. I. Strikman, D. B. Day, and M. Sargsyan, *Phys. Rev. C* **48**, 2451 (1993).
- [11] O. Benhar, D. Day, and I. Sick, *Rev. Mod. Phys.* **80**, 189 (2008).
- [12] C. Ciofi degli Atti and S. Simula, *Phys. Rev. C* **53**, 1689 (1996).
- [13] R. Wiringa, R. Schiavilla, S. C. Pieper, and J. Carlson, *Phys. Rev.* **C89**, 024305 (2014).
- [14] K. S. Egiyan *et al.*, *Phys. Rev.* **C68**, 014313 (2003).
- [15] K. S. Egiyan *et al.*, *Phys. Rev. Lett.* **96**, 082501 (2006).
- [16] N. Fomin *et al.*, *Phys. Rev. Lett.* **108**, 092502 (2012).
- [17] J. Arrington *et al.*, *Phys. Rev. Lett.* **82**, 2056 (1999).
- [18] J. Arrington *et al.*, *Phys. Rev.* **C64**, 014602 (2001).
- [19] J. L. Aclander *et al.*, *Phys. Lett.* **B453**, 211 (1999).
- [20] A. Tang *et al.*, *Phys. Rev. Lett.* **90**, 042301 (2003).
- [21] R. Subedi *et al.*, *Science* **320**, 1476 (2008).
- [22] I. Korover *et al.*, *Phys. Rev. Lett.* **113**, 022501 (2014).
- [23] O. Hen *et al.*, *Science* **346**, 614 (2014).
- [24] E. Piassetzky, M. Sargsian, L. Frankfurt, M. Strikman, and J. W. Watson, *Phys. Rev. Lett.* **97**, 162504 (2006).
- [25] J. Arrington, D. Day, D. Higinbotham, and P. Solvignon, Three-nucleon short range correlations studies in inclusive scattering for  $0.8 < Q^2 < 2.8(\text{GeV}/c)^2$ , 2011.
- [26] J. Alcorn *et al.*, *Nucl. Instrum. Meth.* **A522**, 294 (2004).
- [27] Z. Ye, Ph.D Thesis, University of Virginia, 2013, arXiv:1408.5861.
- [28] D. B. Day, J. S. McCarthy, T. W. Donnelly, and I. Sick, *Annual Review of Nuclear and Particle Science* **40**, 357 (1990).
- [29] S. Stein *et al.*, *Phys. Rev.* **D12**, 1884 (1975).
- [30] A. Aste, C. von Arx, and D. Trautmann, *Eur. Phys. J.* **A26**, 167 (2005).
- [31] J. Arrington *et al.*, *Phys. Rev.* **C86**, 065204 (2012).
- [32] D. W. Higinbotham and O. Hen, *Phys. Rev. Lett.* **114**, 169201 (2015).

- [33] J. Arrington, D. Day, N. Fomin, and P. Solvignon, Inclusive scattering from nuclei at  $x > 1$  in the quasielastic and deeply inelastic regimes, Jefferson Lab Experiment Proposal E12-06-105, 2006.
- [34] J. Arrington, D. Day, D. W. Higinbotham, and P. Solvignon, Precision measurement of the isospin dependence in the 2N and 3N short range correlation region, Jefferson Lab Experiment Proposal E12-11-112, 2011.